SUPPORTING INFORMATION

Detection and Quantification of Biologically Active Botulinum Neurotoxin Serotypes A and B Using a Förster Resonance Energy Transfer-based Quantum Dot Nanobiosensor

Yun Wang,[†] H. Christopher Fry,[‡] Guy E. Skinner,[†] Kristin M. Schill,[†] Timothy V. Duncan[†,]*

† Center for Food Safety and Applied Nutrition, U.S. Food and Drug Administration, Bedford Park, IL 60501

‡Center for Nanoscale Materials, Argonne National Laboratory, Lemont, IL 60439

*Address correspondence to Timothy.Duncan@fda.hhs.gov

ADDITIONAL MATERIALS AND METHODS

Peptide synthesis. BoNT/A specific substrate peptide labeled with BHQ1 (BHQ1-pepA) was prepared using solid-phase peptide synthesis (SPPS) following standard Fmoc chemistry protocols (CS Bio Co. automated peptide synthesizer, CS136XT). Rink amide - MBHA resin (0.25 mmol synthetic scale, loading capacity: 0.39 mmol/g, Chem Impex International, Inc.) was used as the solid support. A solution of 20% piperidine (Sigma-Aldrich) in dimethylformamide (Fisher Chemical, Bioreagent Grade) was used as the deprotecting reagent with subsequent 5 and 20 minute deprotection times. Coupling was executed using four fold equivalents of standard Fmoc protected amino acids (1 mmol, Chem Impex International) and stoichiometric equivalents of diisopropylethylamine (DIEA, 1 mmol, Sigma-Aldrich) and O-Benzotriazole-N,N,N',N'-tetramethyl-uronium-hexafluoro-phosphate (HBTU, 1 mmol, Chem Impex, International, Inc.) in DMF with a 90 minute coupling time. BHQ1 (1 mmol) was double coupled (subsequent 90 minute coupling reactions) to the N-terminus of the peptide using DIEA (1 mmol) and HBTU (1 mmol). Upon completion of the synthesis, the peptide side chains were deprotected and the crude peptide cleaved from the peptidyl resin with a standard trifluoroacetic acid solution (10 mL, 95% TFA, 2.5% triisopropylsilane, 2.5% water) for 3 h. The resulting mixture was filtered into a 20 mL glass vial. The crude peptide was precipitated via dropwise addition of the peptide/TFA solution into cold diethyl ether (90 mL). The suspension was centrifuged followed by decanting of the ether yielding the crude peptide as pellet. The crude peptide was resuspended in water and purified to > 98% purity using reversed phase HPLC followed by lyophilisation to yield the purified peptide in solid form. The sequence is: BHQ1-SNKTRIDQANQRATKMHHHHHH-NH_2. BoNT/B specific substrate peptide labelled with QSY®9 (QSY9-pepB) was synthesized by Bio-Synthesis Inc. (Lewisville, TX), with the sequence of: Ac-LSELDDRADAK(QSY9)QAGASQFETSAAKLKRKYWWKNLKHHHHHH-NH_2. QSY®9 was purchased from its manufacturer by Bio-Synthesis Inc. Both peptides are C-terminal amidated.

QSY9-pepB is N-terminal acetylated. Lyophilized BHQ1-pepA was reconstituted in DMSO to the concentration of 1.6 mM and stored at -20°C. QSY9-pepB was reconstituted in 10% DMSO (v/v in water) to the concentration of 1 mM and stored at -20°C. The peptides were further diluted when needed to required concentrations with assay buffer.

Peptide assembly on QD. The FRET efficiency (*E*) was characterized by changes in QD PL, which was calculated as:

$$E = \frac{PL_D - PL_{DA}}{PL_D} \quad \text{(S1)}$$

where PL_D and PL_{DA} represent the PL intensity peak in the absence and presence of quencher-labeled peptides, respectively. The PL intensity at the peak maximum of QDs not exposed to peptide (2.4 pmol of QD525, or 0.24 pmol of QD585) in 20 mM HEPES buffer (pH 8.0) was designated as PL_D. PL_{DA} was obtained from the PL spectrum of QD (same amount) which was incubated with increasing concentration of corresponding peptide (e.g. QD525 with BHQ1-pepA, and QD585 with QSY9-pepB) in assay buffer for 1 h. Quenching of QDs was observed through the relative PL (S_0/S_B) as:

$$\frac{S_0}{S_B} = \frac{PL_{DA}}{PL_D} \quad \text{(S2)}$$

where S_0 represents the PL signal of the sample with QDs and peptides, and S_B represents PL signal of the sample with only QDs. The optimal peptide concentration was determined as the concentration at which S_0/S_B decreased to <0.1, and levelled off. The optimal reaction time of peptides and QDs was determined by incubating BHQ1-pepA at the optimal concentration with QD525 for 0.5 h to 3 h at room temperature, and QSY9-pepB with QD585 for 0.25 h to 3 h. The Förster critical distance (R_0) was estimated as:

$$R_0 = 0.2108(\kappa^2 \Phi_D n^{-4} J_{DA})^{1/6} \quad \text{(S3)}$$

where κ^2 is the orientation factor (κ^2= 2/3), Φ_D is the quantum yield of the QDs in the absence of quencher, n is the refractive index of the medium (n=1.4), and J_{DA} is the overlap integral. The FRET efficiency (*E*) was also defined as:

$$E = \frac{nR_0^6}{nR_0^6 + r^6} \quad \text{(S4)}$$

where n is the average number of quenchers interacting with each QD, and *r* is the average center-to-center distance from a QD to bound quenchers. Therefore, the average distance between QD and quencher can be estimated as:[1]

$$r = \left[\frac{n(1-E)}{E}\right]^{1/6} R_0 \quad \text{(S5)}$$

Since the actual number of quenchers interacting with QDs was unknown, we used peptide *vs.* QD molar ratio (peptide:QD) to estimate the distance. The FRET efficiency (calculated from experimental data using eq. S1) was fitted with eq. S4, which assumes that the mean QD-quencher distance (*r*) was constant at all peptide:QD ratios.

LcA/B differentiation. The sensor was used to differentiate LcA and LcB in mixed samples. First, a 100 µL sample of LcA and LcB mixture was prepared, containing the two light chains at concentrations listed in Table 1. Half of this mixture was introduced to BHQ1-pepA for 2 or 4 h incubation and then QD525 for one hour incubation, while the other half was introduced to QSY9-pepB (2 or 4 h) and then QD585 (1 h). After incubation, the two halves were combined and adjusted to 200 µL using deionized water. This combined sample was measured with a PL scan from 450 to 660 nm. Negative control samples (0 nM LcA and LcB) were prepared with 100 µL assay buffer and processed the same as the Lc mixed samples. The sensor signal (S/S_0) for each Lc was calculated, and then the concentration was calculated from the S/S_0 using the linear equation obtained from sensitivity tests. The recovery was then calculated by comparing the measured concentrations and the spiked concentrations.

BoNT holotoxin detection. BoNT/A and /B holotoxin were detected using the same method as Lc detection, except that the dilution buffer was supplemented with 0.6 mM $ZnCl_2$ to enhance the activity of the toxin. Due to the possible hazard of the holotoxin, samples were transferred to 96-well flat-bottom plates and sealed with adhesive film for PL measurement.

ADDITIONAL RESULTS AND DISCUSSION

Optimization of peptide:QD ratio and bioconjugation reaction time. The assembly of quencher-labeled peptides on QDs was characterized by measuring the changes in QD PL with increasing peptide:QD molar ratio. Figure S3A presents QD525 PL spectra over a wavelength range of 450 to 600 nm in the presence of various relative concentrations of BHQ1-pepA. Compared to the QD spectrum in the absence of BHQ1-pepA (peptide:QD ratio of zero), the assembly of BHQ1-pepA on the QD surface resulted in a decrease in the QD PL, because the efficiency of FRET is highest when the donor (QD) and acceptor (quencher) are in close proximity (typically, less than ≈10 nm). Figure S3B presents the decrease in QD relative PL (S_0/S_B) and increase in FRET efficiency (E) as the peptide:QD ratio increased. The PL intensity decreased rapidly as the peptide:QD ratio was increased from 0 to 20 (the QD525 content was kept constant at 0.24 pmol); at the higher ratios, the PL intensity leveled off when it was reduced to ≈10% of the original value. The ratio of 20 was used in the LcA detection assay described in the following section to ensure a substantial quenching at the reference point (no BoNT present) but not excessive peptide that could interfere with accurate quantification.

We also investigated how the reaction time between BHQ1-pepA and QD525 affected the FRET efficiency. Figure S3C shows relative PL (S_0/S_B) obtained after reaction times ranging from 30 min to 3 h. The QD PL intensity decreased 85% in the first 1 h of reaction time, and only decreased 5% with an additional 2 h reaction time (up to total of 3 h reaction time). Because additional reaction time beyond 1 h resulted in a negligible increase in quenching efficiency, 1 h was determined to offer a good balance between the desired low PL of the “off” state of the sensor in the absence of target BoNT with a reasonably short total detection time.

Analogous to the BoNT/A probe, the BoNT/B probe design was explored by characterizing the assembly of QSY9-pepB on QD585 via measuring the quenching of QD585 as a function of the peptide:QD ratio and reaction time. As shown in Figure S4A, PL intensity was reduced to ≈10%

of the original emission intensity at the ratio of 100. Compared to the assembly of BHQ1-pepA on QD525, the higher ratio necessary to achieve the same degree of QD585 quenching by QSY9-pepB is mainly due to the larger distance between the QSY9 quencher and the QD585 donor. QD585 is a larger nanocrystal than QD525 (15 *vs.* 12 nm in diameter, as measured from transmission electron microscopy images provided by the manufacturer), and QSY9 is possibly further from the poly(histidine) binding module considering that there are more intermediary amino acid residues than the number situated between BHQ1 and the binding module of pepA.

The larger distance between QSY9 and QD585 (compared to BHQ1 and QD525) was confirmed by the estimated average center-to-center distance (*r*) from the experimental FRET quenching data shown in Figures S3 and S4. The data was fit using eq. S4 to estimate the mean QD-quencher distance (*r*). This equation makes the assumption that *r* does not vary as a function of n (the quencher to QD ratio) (Figure S3B and S4A). It was noted that although the experimental data qualitatively reproduces the trend predicted by eq. S4, there is some discrepancy between the simple FRET model and the experimental data (R^2=0.959 for both quencher-QD pairs). At the range of higher peptide:QD ratio (>15 in Figure S3B, >70 in Figure S4A), QD PL was quenched more than the theoretical FRET value, possibly indicating non-FRET quenching of QD luminescence or that the *r* value is not independent of the n (the quencher to QD ratio). Nevertheless, curve fitting to the simple FRET model (eq. S4) estimated *r* as 112 and 71 Å for the QSY9-QD585 pair and BHQ1-QD525 pair, respectively. It is noted that the interchromophore distance calculation requires knowledge of the number of quencher molecules interacting with each QD; we have used the ratio of peptide:QD as an estimate for this value, which assumes that all quenchers in solution are bound to QDs. This value is higher than the actual number of quenchers tethered to each QD due to the binding efficiency and the purity of quencher-labeled peptide. Therefore, the distance reported above would represent an upper limit to the actual interchromophore distance.

Our evaluation of the BoNT/B sensor also included an optimization of the reaction time. When incubating QSY9-pepB with QD585 at the ratio of 100, the relative PL only decreased 1.8% from 0.5 h to 3 h reaction time, as shown in Figure S4B. Therefore, LcB detection experiments used a reaction time of 0.5 h.

We note that further optimization of the sensor performance may be achieved by purification of the peptide-QD conjugates prior to exposure to toxin. Purification protocols and their potential effect on sensor performance will be reported in a separate report.

Additional information on line fitting for Figures 2 and 4. Figure 2 displayed the LcA sensor signal as a function of concentration. It was noted that the functional relationship was linear over a concentration range of 8 to 200 nM; above this concentration, evidence of saturation of the luminescence signal was observed. In principle, a nonlinear fitting model could be used to extend the quantitative range of the sensor to these higher concentrations, but this would require measuring additional data points at concentrations in excess of 200 nM. It was decided not to undertake this effort because of the unlikelihood of needing to quantify BoNT in foods at such high concentrations. It is possible that other detection scenarios may exhibit saturation effects at lower analyte concentrations, or require detection at higher analyte concentrations than that which is captured by the linear detection range shown in Figure 2B. In such cases, the use of non-linear fitting models may be necessary for accurate quantification over the range of interest.

It is also noteworthy that the linear fit model employed for the data displayed in Figure 2 does not exhibit a y-intercept (S/S_0) value of 1, which would be the theoretical luminescence signal at zero analyte concentration. It was found that forcing the line through the theoretical intercept value resulted in poorer quality fits to the experimental data (as measured by R^2 values). We note that data fitting was only performed for data at analyte concentrations above the LOQ, and that the linear range does not necessarily extend to concentrations lower than this value. Therefore the (extrapolated) y-intercept of the fit line does not necessarily have scientific

relevance and shouldn't necessarily be expected to match the theoretical S/S_0 value at zero analyte concentration.

In the case of data plotted in Figure 4 (for LcB detection), it was noted that at peptide:QD ratios of 100, the relationship between sensor signal and analyte concentration was logarithmic rather than linear. Linear fits to the data when plotted on a logarithmic scale resulted in satisfactory results. When the peptide:QD ratio was increased to 120, a different functionality resulted (see Figure 4C). The fit line in Figure 4C results from a weighted linear fit of the data, where the relative weight of each point was dependent on the standard error. Fits to nonlinear models were also attempted; an example of a polynomial fit to the data is shown in the Supporting Information, Figure S5. For simplicity and consistency, linear functions were generally preferred for estimation of BoNT concentration using the FRET sensors developed here. However Figure S5 shows that in some cases nonlinear fits to the data may result in slight improvements to the accuracy of quantitation at only a small cost to the complexity of data analysis.

SUPPORTING FIGURES

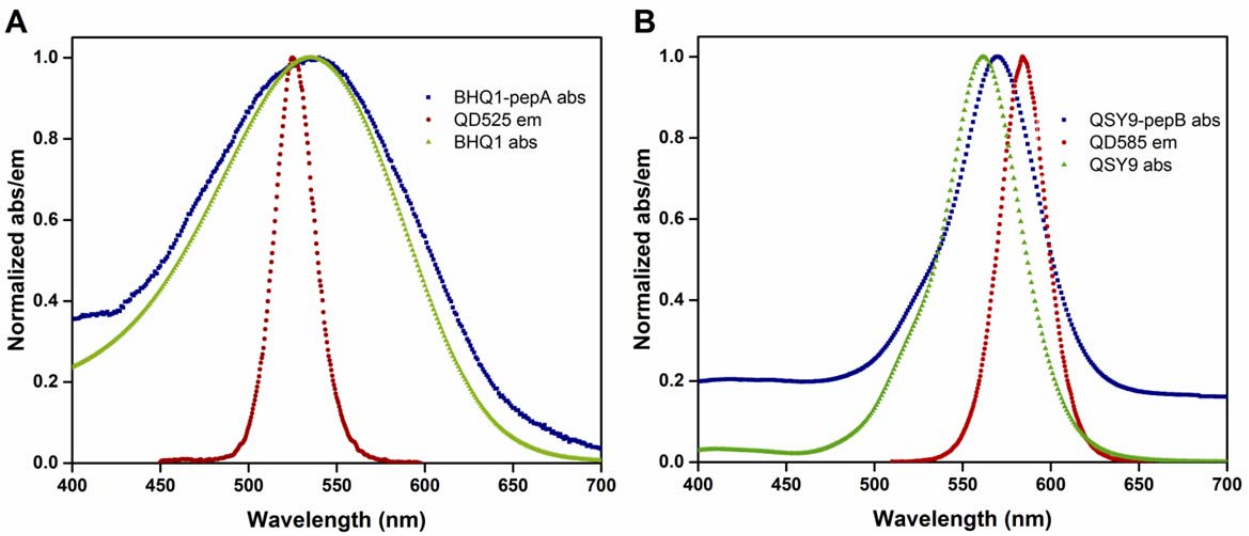

Figure S1. Spectral overlap for the two pairs of donors and acceptors used in the sensor: (A) BHQ1 absorption (abs) and QD525 emission (em); and (B) QSY9 absorption (abs) and QD585 emission (em). The absorption of quencher-labeled peptides is shown as well and no obvious shift in the absorption compared to the corresponding quencher was observed. BHQ1-pepA: BHQ1-labeled peptide for type A detection; and QSY9-pepB: QSY9-labeled peptide for type B detection.

A

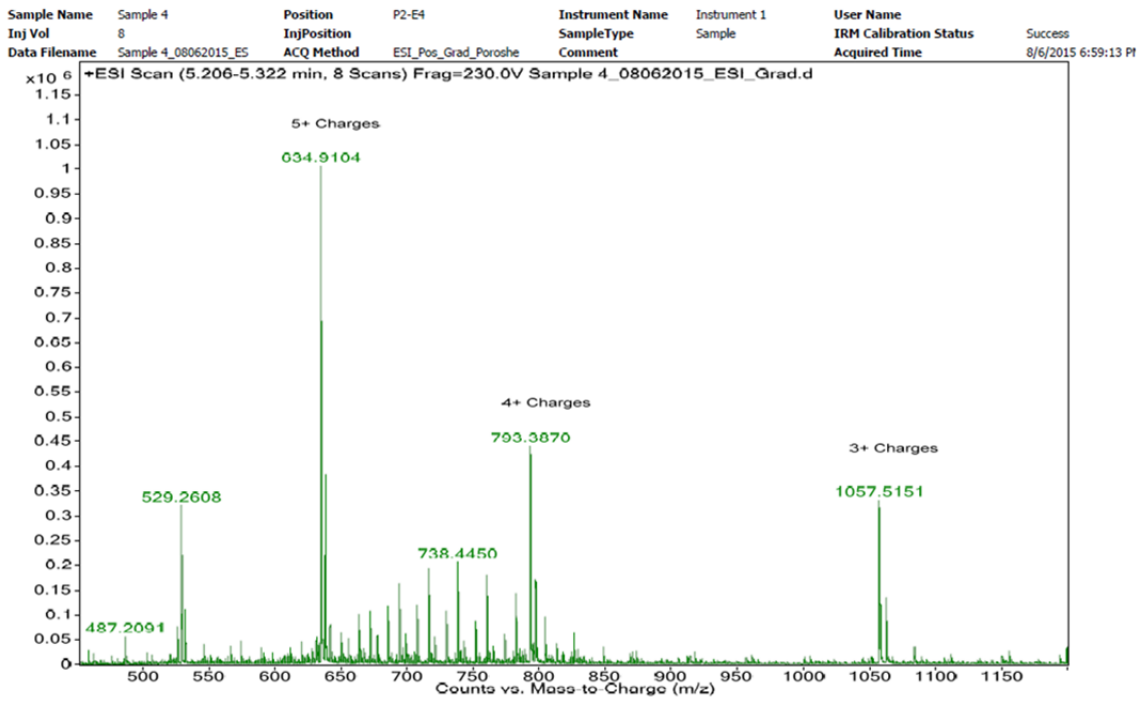

B

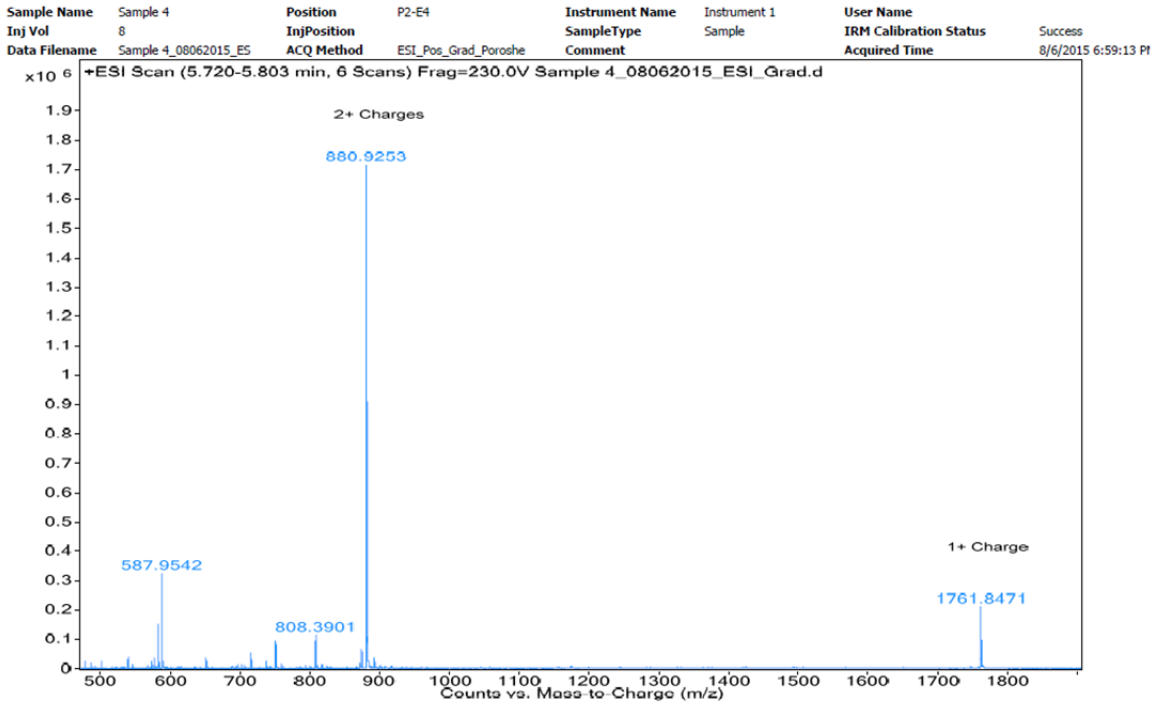

Figure S2. Mass spectra of (A) intact BHQ1-pepA; and (B) BHQ1-pepA N-terminal cleavage product.

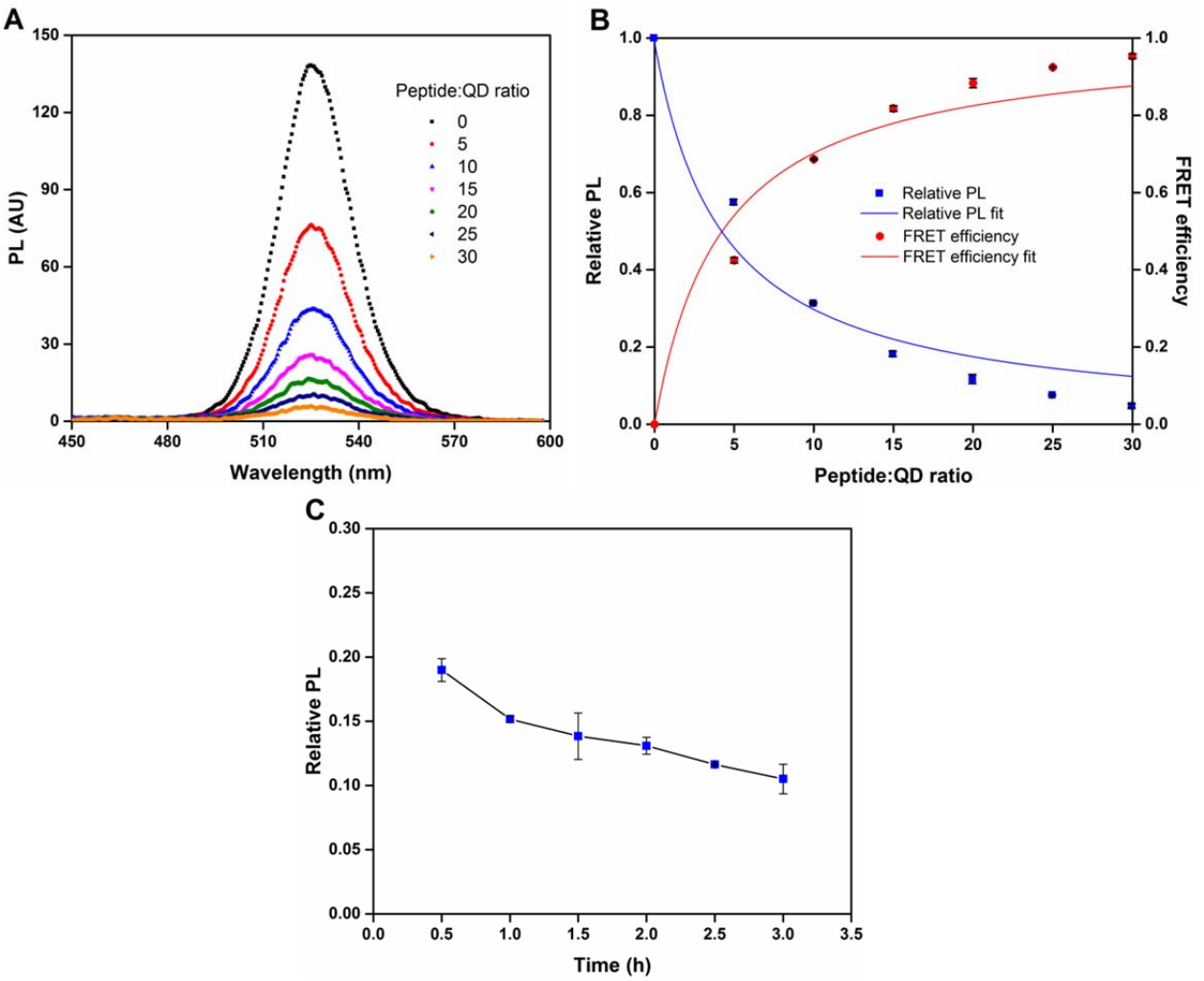

Figure S3. Assembly of black hole quencher 1-labeled peptide for type A detection (BHQ1-pepA) on QD525, as monitored by luminescence spectrophotometry. (A) Photoluminescence (PL) spectra of QD525 as a function of BHQ1-pepA *vs.* QD525 (peptide:QD) molar ratio. The QD PL intensity decreased as the peptide:QD molar ratio (shown in the legend) increased. The peptide was incubated with QD525 for 1 h. Each sample contains 0.24 pmol QD525. (B) Relative PL intensity (blue squares, PL intensity at the QD525 peak maximum normalized to the PL intensity in the absence of BHQ1-pepA) and FRET efficiency (red circles) *vs.* the peptide:QD molar ratio. The data were fit with a simple FRET model (eq. S4; relative PL: blue line; FRET efficiency: red line) (C) Relative QD525 PL after incubating the peptide and QD for times ranging from 0.5 to 3 h. The peptide:QD ratio was 20.

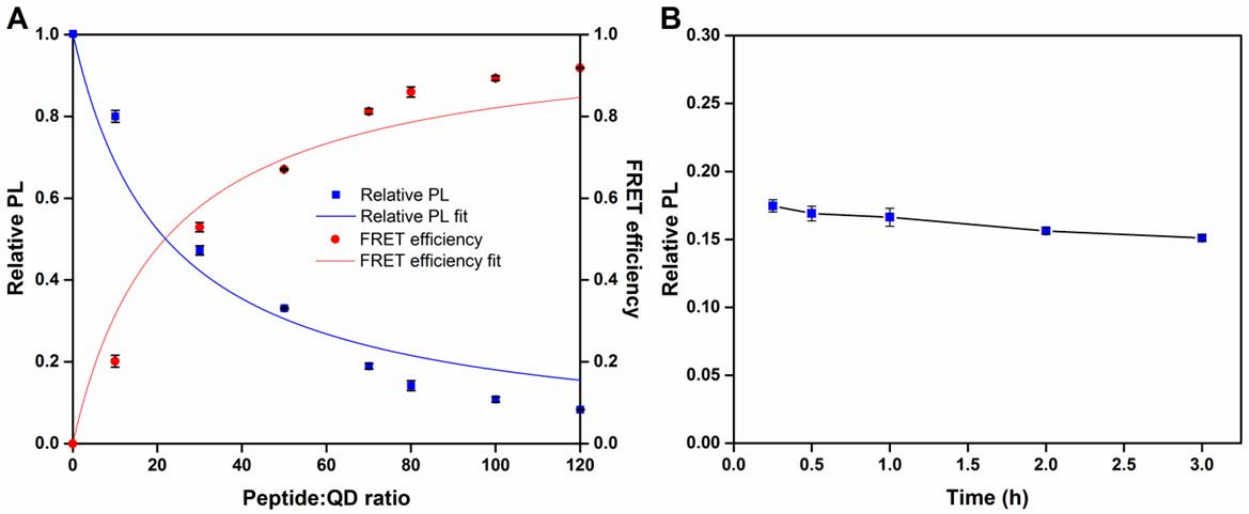

Figure S4. Assembly of QSY9-labeled peptide for type B detection (QSY9-pepB) on QD585, as measured by luminescence spectrophotometry. (A) Relative PL intensity (blue squares, PL intensity at the QD585 peak maximum normalized to the PL intensity of QD585 in the absence of QSY9-pepB) and FRET efficiency (red circles) *vs.* the peptide:QD molar ratio. The peptide was incubated with QD for 1 h. The data were fit with a simple FRET model (eq S4; relative PL: blue line; FRET efficiency: red line). (B) Relative QD585 PL intensity after incubating the peptide and QDs for times ranging from 0.25 to 3 h. The peptide:QD ratio was 100.

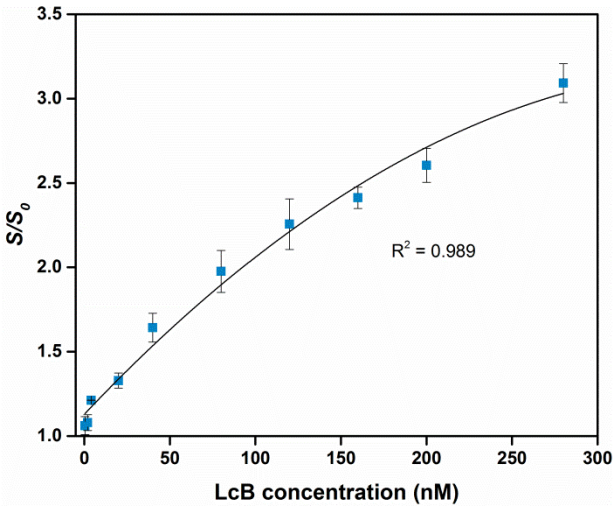

Figure S5. Polynomial fit of the sensor signal *vs.* LcB concentration for LcB detection, with a QSY9-pepB:QD585 ratio of 120, and 2 h LcB and peptide incubation time. Polynomial equation: y= -0.00001x^2+0.0107x+1.1297 (y: S/S_0, x: LcB concentration in nM).

REFERENCES

(1) Clapp, A. R.; Medintz, I. L.; Mauro, J. M.; Fisher, B. R.; Bawendi, M. G.; Mattoussi, H. Fluorescence Resonance Energy Transfer between Quantum Dot Donors and Dye-Labeled Protein Acceptors. *J. Am. Chem. Soc.* **2004,** *126* (1), 301-310.